Metallomics

Accepted Manuscript

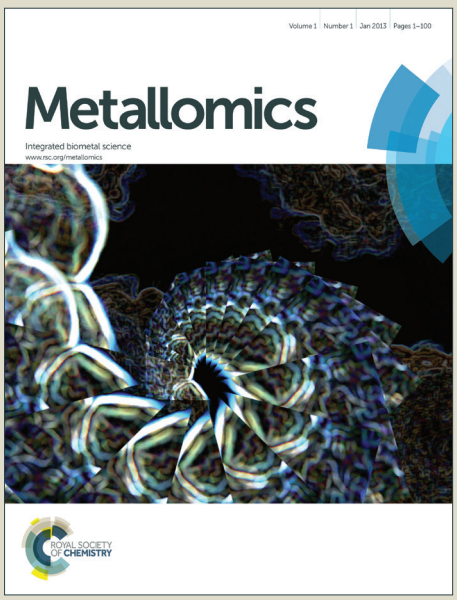

ROYAL SOCIETY OF CHEMISTRY

www.rsc.org/metallomics

Noccaea caerulescens can accumulate more than 2% Zn in the leaves without showing any outwards signs of toxicity however a myriad of elemental and metabolite changes occur at these concentrations.

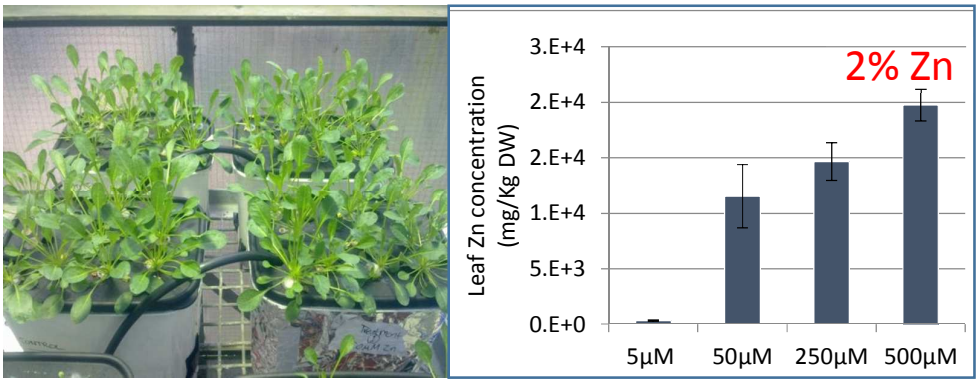

Hyperaccumulation of zinc by *Noccaea caerulescens* results in a cascade of stress responses and changes in the elemental profile

Siavash Foroughi[1], Alan J.M. Baker[1], Ute Roessner[2,3], Alexander A.T. Johnson[1,3], Antony Bacic[2,4,5], Damien L.Callahan[2,6]*

1. School of Botany, The University of Melbourne, Victoria 3010, Australia
2. Metabolomics Australia, School of Botany, The University of Melbourne, Victoria 3010, Australia
3. Australian Centre for Plant Functional Genomics, School of Botany, The University of Melbourne, Victoria 3010, Australia.
4. ARC Centre of Excellence in Plant Cell Walls, School of Botany, The University of Melbourne, Victoria 3010, Australia
5. Bio21 Molecular Science and Biotechnology Institute, The University of Melbourne, Victoria 3010, Australia
6. Centre for Chemistry and Biotechnology, School of Life and Environmental Sciences, Deakin University, Victoria 3125, Australia

* Corresponding author: Tel.: +61 3 92517422

E-mail address: damien.callahan@deakin.edu.au (D. L. Callahan)

Running title: Metabolomics of Zn hyperaccumulation

Key words: *Noccaea caerulescens*, Zinc, hyperaccumulation, metabolomics, stress signalling, elemental profiles, Zn-complex

ABSTRACT

Noccaea caerulescens (J. & C. Presl) F.K. Meyer is a metal hyperaccumulating plant which can accumulate more than 2% zinc (Zn) dry tissue mass in its aerial tissues. At this concentration Zn is toxic to most plants due to inhibition of enzyme function, oxidative damage and mineral deficiencies. In this study the elemental and metabolite profiles of *N. caerulescens* plants grown in four different Zn concentrations were measured. This revealed broad changes in the metabolite and elemental profiles with the hyperaccumulation of Zn. The Zn treated plants exhibited no typical signs of stress such as chlorosis or reduced biomass, however, a range of metabolic stress responses, such as the modification of galactolipids, major membrane lipids of plastids, increases in oxylipins, which are precursors to the signalling molecules jasmonic and abscisic acids, as well as the increased synthesis of glucosinolates, was observed. Increases in particular organic acids and the ubiquitous metal cation chelator nicotianamine were also observed. The small molecule metabolite changes observed, however, did not account for the extreme Zn concentrations in the leaf tissue showing that the increase in nicotianamine production most likely negates Fe deficiency. The elemental analyses also revealed significant changes in other essential micronutrients, in particular, significantly lower Mn concentrations in the high Zn accumulating plants, yet higher Fe concentrations. This comprehensive elemental and metabolite analysis revealed novel metabolite responses to Zn and offers evidence against organic acids as metal-storage ligands in *N. caerulescens*.

INTRODUCTION

Transition metals such as Mn, Fe, Ni, Cu and Zn are essential components of many enzymes and are necessary for plant and animal survival. The fundamental properties of transition metals include their high affinity for molecules containing nitrogen, oxygen and sulphur, and their access to different redox states under physiological conditions. These properties, however, also render the metal ions extremely toxic at higher concentrations as they can interfere with redox balance, enzyme function and nitrogen metabolism, inhibit mitotic activities, cause oxidative damage and reduce the uptake of other essential micronutrients.[1-5] For these reasons metal ion homeostasis must be tightly controlled. Some plants, however, have evolved the ability to not only survive in metal-rich soils but to also sequester and store exceptionally high levels of metals in their aerial tissues at concentrations which would be toxic to most plant species.[6] These *hyperaccumulators* have developed unique molecular mechanisms which prevent them from succumbing to the toxic effects of high metal ion concentrations, however, the mechanisms employed by hyperaccumulators to resist metal-ion stress are still poorly understood. Hyperaccumulation requires alterations to several physiological parameters including metal ion transport systems, membrane structure and function and tissue water content as well as global changes to gene expression, protein, lipid and metabolite profiles.[7] There are at least four key pathways proposed for metal hyperaccumulation in leaf tissue: (i) metal influx across the root cell plasma membrane, (ii) reduced metal sequestration of metal ions into root vacuole (iii) increased metal xylem loading for transport to leaf tissue followed by, (iv) metal influx across the leaf cell plasma membrane and storage in the leaf vacuole.[8]

More than 500 plant taxa that hyperaccumulate one or more heavy metals and metalloids have so far been identified.[7] These plants have been described from metalliferous soils in

disparate geographical regions.[9] The uptake and hyperaccumulation of metals is an active trait that has evolved possibly as a defence mechanism against predators and disease.[10] Hyperaccumulators provide a unique model which can be used to increase our understanding of how plants maintain metal ion homeostasis. One feature of hyperaccumulation is the constitutive expression of a plethora of both metal-chelator biosynthetic and metal transporter genes.[11] For example, gene expression studies in *N. caerulescens* have shown constitutive high expression of the Zn transporter gene *ZNT1* in root cells when compared to closely related non-accumulating species.[12, 13]

There has been much focus on revealing the metabolic responses of plants to environmental stresses such as drought, salinity and heat, however our understanding of how plants respond to the presence of heavy metals at the metabolome level is limited[14] The metal ions in aerial tissues must be sequestered and stored in non-labile inert metal complexes or sub-cellular structures. It is thought that organic acids play a key role in metal ion sequestration in the leaves of hyperaccumulators.[15-19] It is not known, however, if the associations observed between the accumulated metal ions and organic acids are truly part of the overall detoxification mechanism. Organic acids have relatively low association constants (K) with transition metal ions, for example, the complex of citric acid and Zn has a K = 5.0 compared with the ubiquitous metal cation chelator nicotianamine which has a K = 15.4, 10 orders of magnitude higher.[20-22] The presence of relatively labile metal-organic acid complexes does not explain how plants resist protein damage and oxidative stress as the metal ions are not sequestered in inert complexes under physiological conditions.

This study focuses on the Zn, Cd and Ni hyperaccumulating species, *Noccaea caerulescens* (formerly *Thlaspi caerulescens*), which in recent years has been at the forefront of research

concerning hyperaccumulation and has been recognised as a model species to study hyperaccumulation.[7, 8, 23, 24] *Noccaea caerulescens* is a member of the Brassicaceae family and is thus related to *Arabidopsis thaliana* sharing around 88% sequence identity in DNA coding regions.[25] Using a proteomics approach a recent study on *N. caerulescens* showed that epidermal cells have increased capability for coping with oxidative stress and that epidermal cells have greater abundance of a Zn influx transport protein of the ZIP family.[26] The current study employed an untargeted metabolomics approach to analyse changes in the metabolite profiles in leaves of *N. caerulescens* plants which have hyperaccumulated Zn. Furthermore, the full elemental profile was measured in order to investigate possible associations between elemental and metabolic changes that occur during hyperaccumulation of Zn in *N. caerulescens*.

MATERIALS AND METHODS

Plant growth and harvesting.

Seeds of *N. caerulescens* (Bradford Dale population, Derbyshire, U.K.)[27] were surface sterilised in 70% (v/v) ethanol for 5 mins followed by 3 washes with deionised water. Seeds were then immersed in 10% (v/v) sodium hypochlorite and 2% (v/v) Tween 20 solution for 10 mins with agitation before a further 6 washes in deionised water. This procedure was carried out in a laminar flow cabinet to ensure sterile working conditions.

Seeds were placed on moistened filter paper in Petri dishes, and incubated in the dark for 3 days. Seedlings were grown for 6 days until at a height of ~2 cm before transfer to 2 L plastic hydroponic containers filled with 1/5-strength Hoagland's solution (Table S1). Plants were grown in a glasshouse (25ºC/20ºC, 14 hrs/10 hrs light/dark) for a total of 16 weeks. The nutrient solutions were aerated continuously and changed weekly. After 8 weeks of plant growth, 4 treatments comprising one unamended control (containing 5 μM Zn) and three treatments of 50, 250 and 500 μM Zn were employed with 10 plants per treatment from the same seed population, a total of 40 plants for the experiment. Concentrations used were based on reported levels of Zn accumulation in *N. caerulescens* from a 500 μM amended nutrient solution.[28] Shoot tissue was harvested after 16 weeks of growth (Figure 1). To quench metabolism leaf tissue was immediately frozen in liquid nitrogen then the total shoot biomass was accurately weighed and recorded. The tissue from each plant was then homogenised by grinding in liquid nitrogen with a pestle and mortar then stored at -80°C until analysed.

Elemental analysis by ICP-OES

Approximately 100 mg fresh weight (FW) of the homogenised shoot biomass was taken from each plant and dried at 50°C until a constant dry weight (DW) was observed. Dried and ground leaf material was accurately weighed (~15 mg) and acid digested at 70°C for 3 hours in Eppendorf tubes (2.5 mL) with concentrated HNO_3 (0.3 mL). The resulting clear acid

digests were transferred to 10 mL volumetric flasks and made to volume with deionised water. Acid digest were analysed with a Varian Vista inductively coupled plasma atomic emission spectrometer (ICP-OES; Varian Inc., Melbourne, Victoria, Australia) with the following settings: power 1 kW, plasma flow 15 L/min, auxiliary flow 1.5 L/min and nebuliser flow 0.9 L/min. Instrument data were evaluated using Vista Pro ICP expert 4.1.0.

The instrument was calibrated with standard solutions of Al, As, B, Cd, Cr, Cu, Fe, Hg, K, Pb, Co, Mn, Na, Ni, P Se, V, Zn ranging between 5 mg/L and 100 mg/L. These solutions were prepared by appropriate dilutions with deionised water of the ICP mixed element stock standard (AM3, Choice Analytical, Australia) and B, K, Na, P (Choice Analytical, Australia) stock standards.

LC-MS tissue extraction, instrument details and data analysis.

Six extraction protocols were evaluated: (1) Hot methanol (MeOH) (70°C) then water; (2) acetonitrile then water; (3) 2/3/3 water/acetonitrile/isopropanol; (4) 50% MeOH; (5) hot MeOH then water/chloroform; (6) 0.1% formic acid ice cold MeOH. Protocol (3) provided the most complete coverage of polar and non-polar molecular features on a reversed phase chromatography column. Homogenized leaf tissue (50 mg) was accurately weighed into 2 mL cryomill tubes containing ceramic beads. The internal standards $^{13}C_6$ ^{15}N valine and 2-aminoanthracine, was added (10 µL of 1.5 mM mixed standard, final concentration 20 µM) then samples extracted with 250 µL 2/3/3 water/acetonitrile/Isopropanol using the Preselys cryomill with the following settings: temperature 5°C, speed 3,800 rpm, time 3 × 30 s. Tubes were centrifuged and supernatant removed. The pellets were then re-extracted as just described. The supernatants were pooled and transferred to 2 mL vials for analysis.

An Agilent 1200 series liquid chromatography (LC) system (maximum pressure 600 bar) comprising a vacuum degasser, binary pump, column oven and temperature controlled

autosampler was interfaced with a dual electrospray ionization quadrupole time of flight mass spectrometer. (ESI-QTOF-MS; Agilent 6520). The LC parameters were as follows: column 2.1 × 100 mm, 1.8 µm C18 Zorbax Elipse plus (Agilent), column temperature 30°C, flow rate 0.4 mL/min, with gradient elution. Mobile phase A 0.1 % formic acid in water, mobile phase B 0.1% formic acid in acetonitrile. The initial mobile phase composition was 2%B which was changed linearly to 100%B over 10 minutes with a 2 minute hold at 100% B then re-equilibration for 5 min at 2% B, giving a total run time of 19 mins. The ESI source settings were: gas temperature 300°C, gas flow rate 10 L/min, nebulizer pressure 45 psi, capillary voltage 4000 V, fragmentor 150 V. Reference ions 121.0508 *m/z* and 922.0097 *m/z* for in-spectrum calibration were supplied through the second ESI needle. Instrument was tuned in extended dynamic range mode and spectra collected between 70-1700 *m/z* at 2 scans/second. Injection order was randomized and instrument mass accuracy was recalibrated every 20 samples with blanks injected after re-calibration. No injection order bias was observed (Figure S1). This method resulted in typical chromatographic peak widths of 6 seconds. Retention time variation was 0.13 mins and mass accuracy varied from -0.23 – 2.16 mDa (based on the internal standards).

The LC-MS metabolite peak lists were created for each sample using the 'Find by molecular feature' function in the MassHunter software (Agilent Technologies) which creates a peak list containing the accurate mass, retention time and abundance for each metabolite in the sample. Retention time alignment, metabolite identification based on the information described above, data transformation and statistical analysis was carried out using Mass Profiler Professional software (Agilent Technologies). The MassHunter quant software was also used to target key metabolites identified using Mass Profiler Professional.

GC-MS tissue extraction & derivatisation and instrument details

Approximately 60 mg (accurately weighed and recorded) of frozen homogenised leaf tissue was transferred into cryo mill tubes and extracted with 100% methanol (500 µL) and further homogenised using a cryo mill (Bertin Technologies, France). Samples were extracted for 15 min at 70°C in a thermomixer at 750 rpm, followed by centrifugation for 10 min at 14,000 rpm. Supernatants were removed and extraction process was repeated with 50% methanol and internal standards mixture (1 nmol ^{13}C labelled sorbitol and 10 nmol ^{13}C ^{15}N labelled valine). The supernatants were pooled and stored at -80°C until analysis.

A standard two step derivatisation process of methoximation followed by silylation of metabolites was used to facilitate volatilisaton and improve thermal stability. Methoxyamine hydrochloride (40 µL; 30 mg/mL in pyridine) was added to dried aliquots and incubated for 120 min; 37ºC. This was followed by the addition of with N-methyl-N-(trimethylsilyl)trifluoroacetamide (70 µL; TMS) and a further incubation at 37ºC for 30 min. A retention time standard mixture (5 µL, 0.029% (v/v) *n*-dodecane, *n*-pentadecane, *n*-nonadecane, *n*-docosane, *n*-octacosane, *n*-dotracontane, and *n*-hexatriacontane dissolved in pyridine) was added prior to trimethylsilylation. Samples (1 µL) were then injected via the splitless mode onto a GC column a hot needle technique.

The GC-MS system used comprised of a Gerstel 2.5.2 autosampler, a 7890A Agilent gas chromatograph and a 5975C Agilent quadrupole mass spectrometer (Agilent, Santa Clara, USA). The mass spectrometer was tuned according to the manufacturer's recommendations using *tris*-(perfluorobutyl)-amine (CF43). GC was performed on a 30 m VF-5MS column with 0.25 µm film thickness with a 10 m Integra guard column (Varian, Inc, Victoria, Australia). The injection temperature was set at 250°C, the MS transfer line at 280°C, the ion source adjusted to 250°C and the quadrupole at 150ºC. Helium was used as the carrier gas at a flow rate of 0.8 mL/min. The analysis of TMS samples was performed under the following

oven temperature program; start at injection 70°C, a hold for 1 minute, followed by a 12.5°C min^{-1} oven temperature ramp to 325°C and a final 6 minute heating at 325°C. The system was temperature equilibrated for 1 minute at 70°C prior to injection of the next sample. Mass spectra were recorded at 2 scan s^{-1} with an *m/z* 50-600 scanning range.

GC-MS data processing and statistical analysis

The chromatographic deconvolution software, PyMS was used with the following settings: window for peak picking = 13 scans, scans to combine to correct for spectral skewing = 2, required number of ions over threshold = 3.[29] Mass spectra of eluting TMS compounds were manually identified using the commercial mass spectra library NIST (http://www.nist.gov), the public domain mass spectra library of Max-Planck-Institute for Plant Physiology, Golm, Germany (http://csbdb.mpimp-golm.mpg.de/csbdb/dbma/msri.html) and the *in-house* Metabolomics Australia mass spectral library. All matching mass spectra were additionally verified by determination of the retention time by analysis of authentic standars. Relative response ratios were calculated using the metabolite peak area normalized to the sample mass (g) and internal standard area, as described by Roessner *et al.*[30] Statistical analysis was performed using R statistical software package (R version 2.12.0). Analysis of Variance (ANOVA) was used to test for significance between ion concentrations, while the t-test was used to determine statistically significant changes in metabolite concentrations. Differences between observations are described as statistically significant (where $P<0.05$).

RESULTS

Plant growth and elemental analysis by ICP-OES.

No visible symptoms of Zn toxicity, such as chlorosis and inward-rolled leaf edges, were observed in any of the 40 plants grown for this experiment (Figure 1). Further, there were no

significant differences (ANOVA: $P>0.05$) in the total fresh leaf tissue mass (Figure S2). These results are consistent with those of previous studies performed under similar growth conditions.[26, 31, 32]

As expected large and statistically significant increases in Zn concentrations were found in the treated plants when compared to the control group ($P < 0.001$; Figure 2A). The leaf Zn concentrations were above the Zn accumulation threshold of 3,000 mg kg^{-1} for all plants supplemented with extra Zn.[6, 33] These data were consistent with the findings of Baker *et al*.[27] A 37-fold increase in the Zn concentration was observed in the 50 μM Zn treated plants. The highest Zn treatment (500 μM) resulted in a mean Zn concentration of 19,750 mg kg^{-1} dry mass, or a 64.4 fold increase from the control (Figure 2A). Our data suggest that the plants were reaching an accumulation maximum as only 1.7- and 1.3-fold increases were observed when comparing the highest treated plants to the 50 and 250 μM treatments, respectively.

For the other elements measured statistically significant changes in B, Na, Cu, Mn, and Fe were observed between treatment groups when compared with the control (Figure 2B). Of particular note was the Mn concentration which was 2.5- and 4.0-fold lower in the 250 μM and 500 μM Zn treated plants, respectively (Figure 2B). Fe concentrations were the highest in the highest treatment concentration, with 1.30-fold higher concentrations relative to the control plants. In comparison to the control, B and Cu had significant decreases only at the high and medium treatment groups. With Na, the 50 μM treated plants had the highest concentrations then levels returned to the similar concentrations observed in the control plants.

Metabolite analysis

Two analytical techniques, gas chromatography-mass spectrometry (GC-MS) and liquid chromatography-mass spectrometry (LC-MS), were used to analyse the leaf metabolome. These two analytical techniques are complementary. GC-MS analysis of TMS derivatised extracts is suited to highly water soluble primary metabolites such as small organic acids, amino acids and sugars. Reversed-phase (RP) LC-MS with gradient elution enables the analysis of molecules with a certain degree of hydrophobicity, such as some organic and amino acids, secondary metabolites such as glucosinolates, polyphenols and lipids. A comparative analysis was carried out on the four Zn treatment groups *i.e.* control (5 µM), 50 µM, 250 µM and 500 µM, to identify metabolites changes in response to the presence of increasing Zn concentrations within the leaf tissue.

LC-MS results

A high resolution QTOF-MS was used to collect C18 RP LC-MS profiles in both positive and negative ionisation modes. These metabolite profiles represent a broad sub-set of the metabolome. The retention time, accurate mass, isotope pattern, mass defect, formation of negative/positive ion and fragmentation patterns and library matching allows putative identification, *i.e.* identification without standards, of eluting metabolites. For example, amino acids and Zn ions elute between the un-retained fraction between 0-1 min (Figure 3). The isotope pattern for Zn is distinctive (Figure 4) and complexes with Zn are charged and generally polar thus eluting in the void volume. Secondary metabolites, such as flavonols and glucosinotates, have some degree of hydrophobicity and elute in the middle part of the elution gradient between 1-7 min, while lipids with a high degree of hydrophobicity elute at the end of the LC gradient between 7-14 min. The aligned peak matrices contained 1,688 and 717 mass features in the positive and negative ionisation mode, respectively (Table S2). A principal components analysis (PCA) of these data shows distinct grouping (Figure 5) of the

treatment groups with a clear trend from low to high Zn treated plants. In the positive ion mode data 147 mass features had a statistically significant fold change of greater than 1.5 ($p<0.05$, $n=10$) in the 500 μM Zn-treated plants in relation to the controls. Of the 147 mass features 54 could be identified. These mass features have been grouped into chromatographic elution zones to aid the description (Figure 3). Between 0-1 min 17 of the 147 metabolites showed significant changes with the majority attributed to Zn-containing ions. These were identified by the characteristic isotope pattern (Figure 4). These highly polar and charged Zn complexes probably do not represent the *in vivo* complexes since these metal complexes are able to dissociate or form during extraction and chromatographic fractionation. Furthermore, due to the large number of co-eluting compounds in the void volume, complexes can be formed in the ionisation source, for these reasons, identification of the Zn-complexes was not pursued.

In the region of the chromatogram between 1-7 min 29 metabolites showed significant changes and could be attributed to secondary metabolites and small peptides but few these metabolites were able to be assigned an identity.

A large proportion (42%) of the metabolites contributing to the grouping in the PCA are attributed to the galactolipids, monogalactosyl diacyglycerol (MGDG) and digalactosyl diacylglycerol (DGDG), and the oxidised forms of these lipids which eluted between 7-14 mins (Figure 6). These species match the MS and MS/MS fragmentation patterns (Figure 7) reported by Ibrahim *et al.* 2011 as well as the accurate mass (0.6 ppm mass difference), the isotope pattern for the theoretical structure and the chromatographic elution order described by Ibrahim *et al.* 2011 which used similar chromatography.[34] MGDG and DGDG typically constitute 80% of thylakoid membrane lipids and about 60% of all leaf lipids.[35] With the increased concentration of oxidised galactolipids a corresponding decrease in abundance of the non-oxidised forms was also observed (Figure 6). It is important to note that the levels of

arabidopsides increased significantly more in the highest Zn-treated plants, for example with arabidopside A, a 5.9-fold increase was observed from the 250 to 500 μM Zn treatment compared with a 1.6-fold increase from the 50 to 250 Zn treatment.

A PCA of the negative ion mode data showed a similar trend to the positive ion mode dataset (Figure S3). Of the 717 mass features 71 showed a statistically significant fold change of 1.5 ($P<0.05$, $n=10$). In the region of the chromatogram between 0-1 min 17 mass features attributed to Zn-complexes and organic acids were identified. The increases in organic acids agree with previous observations made for citric acid, malic acid and nicotianamine (Figure 8).[26] However, no Zn complex with citric acid was detected, only with malic acid (Figure 4).

Further evidence of signalling molecules and defence response was detected in the negative ion mode data set. In the region of the chromatogram between 1-7 min 29 mass features were significantly changed. More than 120 glucosinolates have been identified in the Brassicaceae.[36] Using accurate mass, isotope pattern and expected retention time six glucosinolates were identified as having significantly increased with Zn treatment (Figure 8). The most significant was 4-methylsulfinylbutyldesulfo-glucosinolate which was 2.5-fold higher in the 500 μM treated plants compared to the controls as well as increases across all treatments. Plants in the Brassicaceae constitutively contain glucosinolates which make up part of the defence mechanisms against herbivores and microorganisms and are also induced to higher levels through physical damage to the plant.[37, 38] No changes in identified polyphenols were observed in response to the Zn treatments.[39]

In the region of the chromatogram between 7-14 min 24 mass features were significantly changed, some attributed to galactolipids. The precursor to jasmonates, *cis*–(+)-12-oxo-phytodienoic acid (OPDA), increased by 1.8-fold for the 500 μM treated plants when compared to the average of the control plants. OPDA is a lipid derived oxylipin that is found esterified to galactolipids.

GC-MS results

Chromatographic deconvolution of the TMS derivatised metabolites detected 454 chromatographic peaks. Of these, 75 were identified using the commercial NIST and in-house database (Table S3). As with the LC-MS data, a PCA of all 454 peaks shows clear separation of each treatment group and tightness within group clustering (Figure S4). Investigation of the loadings plot revealed that the majority (84%) of the metabolites which explain the separation were unidentified. This illustrates a limitation of GC-MS as unmatched compounds cannot be identified using approaches available to ESI-MS data. The majority of the changes occurring cannot be described and therefor only a selective description of the results can be made based on the compounds identified. A PCA of only identified metabolites still showed clear grouping (Figure S4). A summary of the metabolites resulting in the grouping is in Table S3. Gluconic acid, citric acid, asparagine and GABA contributed most significantly in the separation of the treated groups from the control. Histidine has previously been shown to coordinate intracellular Zn in roots of *N. caerulescens* as well as a smaller proportion coordinating with Zn in the cell wall of leaf tissue.[16] In our experiments, all Zn treatment groups under study exhibited a small decrease in histidine abundance when compared with control plants suggesting no role of histidine and Zn co-ordination in the leaves.

DISCUSSION

Elemental changes

The changes in transition metal concentrations observed may be explained by the Irving-Williams series of first-row transition metals complexes.[40] The relative stability of metal-ion complexes typically follow the trend: Mn(II) < Fe(II) < Co(II) < Ni(II) < Cu(II)> Zn(II) and the order of chlorosis induction has been shown to generally follow this series.[40, 41] The reduction in Mn concentration with higher Zn treatments provides evidence that metals are

transported to the leaves in metal complexes and not as free hydrated cations. As Zn^{2+} forms more stable complexes than Mn^{2+} the Zn^{2+} ions will be chelated and transported to the leaves in place of Mn^{2+} resulting in lower Mn leaf concentrations. It could be hypothesised that *N. caerulescens* has the ability to negate chlorosis by increasing the ability to transport Fe. An increase in the metal cation chelator, nicotianamine, was observed in the metabolite data as well as previous studies.[26] Other studies have shown reduced Zn accumulation in *Arabidopsis halleri* plants with reduced root nicotianamine levels suggesting nicotianamine plays an important role in the symplastic transport to the xylem within the roots.[42] It has also been shown that changing expression level of NA in *A. thaliana* effects the partitioning of Zn and Fe throughout the plant.[43] The 2.7-fold increase in nicotianamine concentration, however, does not match the 64-fold increase in Zn concentration suggesting that nicotianamine is not involved in Zn storage, rather, the increase is more likely a mechanism used for transport to maintain and/or increase concentrations of other metal micronutrients under Zn hyperaccumulation, in particular Fe with no effect on Mn concentration. The ability of *N. caerulescens* to negate Fe deficiency in the presence of extreme Zn concentrations represents a key adaption to the plants ability to hyperaccumulate transition metals without suffering from chlorosis.

Stress responses in response to Zn accumulation

The metabolite analysis supports the findings by Schneider *et al.* 2013 where a higher abundance of proteins involved in the response to oxidative stress was found.[26] Oxidised galactolipid species were first identified in *A. thaliana* and they are now collectively known as arabidopsides.[44, 45] The oxidised products of galactolipids typically contain a cyclopentenone moiety, for example, 12-oxo-phytodienoic acid which is esterified to the glycerol backbone at one or both positions or the sugar moiety of the galactolipid (Figure

7).[34] The biochemical role of arabidopsides is still unknown. Studies have suggested that these lipids may act as signalling molecules[44, 46, 47], may inhibit root growth[48], promote leaf senescence[49] and have antimicrobial functions[50] which are all wounding or stress related responses. The detection of free OPDA is further evidence of stress signalling related to the arabidopsides. The oxylipin derived hormones, such as jasmonic acid, have been shown to interact with proteins in order to influence gene transcription.[51] However, researchers have been careful to point out the difficulty in determining the function of these lipid signalling molecules.

Salicylic acid levels did not change in response to Zn. This was also observed by Fones et al. 2013 who proposed there is an alternative (unknown) defence signalling pathway present in *N. caerulescens* which is decoupled from signalling via reactive oxygen species.[52] Additional support for this hypothesis was found in a study on the closely related Cd hyperaccumulator *Noccaea praecox* where an increase in jasmonic acid was found with Cd treatment.[53]

Furthermore, the induction of glucosinolates synthesis observed has been found to be mediated by jasmonate signalling and could therefore be part of the stress signalling mechanism.[37] In the future it will be important to determine the function of these lipid mediators and, in particular, explore the hypothesis that the oxylipins interact directly with proteins

Primary metabolites

It is important to highlight that the Zn treated plants had between up to 70 times the concentration of Zn in comparison to the controls however no relative increases of the same magnitude were observed in any single primary metabolite identified by GC-MS. Either these small metabolites are constituatively high in concentration in *N. caerulescens* in relation to non-accumulating plants or they are not involved in hyperaccumulation. Previous studies

have shown that *N. caerulescens* leaves contain constitutively high malate and citrate concentrations.[28, 54, 55] This was also observed in these data suggesting that the constitutively high organic acid concentration may require *N. caerulescens* to have high Zn and Fe tissue concentrations for optimal growth.

Sugars such as glucose, sucrose and raffinose are known to accumulate in plant cells under abiotic stress conditions.[56] In this study there was no observed increase in these sugars. Gluconate levels in the leaves of Zn-treated *N. caerulescens*, on the other hand, displayed large changes with a maximum increase of 34-fold seen in the high Zn treatment group when compared to the control plants. Gluconate is a known metal chelator and could either perform a role as a metal transport ligand or osmoprotectant which may help stabilise cell membranes and proteins. The role of gluconate needs to be further explored in *N. caerulescens*.

Only two amino acids, GABA and methionine, as well as putrecine showed increased abundance by GC-MS. Speculative functions have been attributed to GABA metabolism in plants such as osmoregulation,[57] glutamate homeostasis control[58] and salt tolerance in *A. thaliana.*[59] The upregulation of methionine in response to Zn is significant. Previous studies have shown a strong correlation between Ni and nicotianamine in *Noccaea.*[60] Nicotianamine is produced through the condensation of three S-adenosylmethionine molecules catalysed by nicotianamine synthase,[61] therefore the increase of methionine may coupled to the increased nicotianamine synthesis observed.

Zn-complexes in *N. caerulescens*

Localisation studies using X-ray based micro-analytical techniques have shown that Zn is bound to oxygen containing ligands, such organic acids or the plant cell wall in the epidermal leaf cell vacuoles of *N. caerulescens.*[16, 18, 62] However, absolute identification of the co-

ordination chemistry of Zn *in vivo* is challenging. Other researchers have studied ligand exchange with organic acids and nicotianamine using ESI-MS.[63] Rellán-Álvarez *et al.* [63]concluded that citric acid replaces nicotianamine at pH 5.5 (the vacuole pH) and some acceptance of this theory based on citrate replacing nicotianamine within the vacuole has emerged.[26, 64] However, this ligand exchange is considered unlikely to occur in solution. The formation of transition metal complexes depends on both the pH and the equilibrium concentrations of the metal-cation and ligand. During ESI these equilibria change and therefore the detected complexes do not necessarily reflect the solution phase co-ordination chemistry.[65] Since the association constant for nicotianamine is 9-orders of magnitude higher than citric acid a 1.5-fold change in acid concentration could not result in the dissociation of nicotianamine in the vacuole.

As discussed the presence of a Zn complex in the ESI-MS does not necessarily reflect the Zn complex in the leaf. A mass balance calculation based on the amount of Zn in the leaves shows that a very high concentration of any single metal-binding ligand would be required to chelate all accumulated metal-ion. The mean concentration of Zn in the highest treated plants was approximately 20,000 mg/kg or 2 g/100 g. This is equivalent to 0.0306 mol of Zn per 100g leaf dry matter. If nicotianamine is the storage ligand in a 1:1 complex, the total mass of this complex would be 11.27 g or 11% of the total leaf dry mass. Considering that some observations show that Zn is predominantly in the epidermal vacuoles and not uniformly distributed in the leaf then this value would be even higher. A 1:1 complex with citrate would result in 8% of the total leaf mass or 13% in a 1:2 M:L complex. These mass balance calculations suggest that it is unlikely that Zn is bound in a small organic complex and that other storage mechanisms are in play.

CONCLUSIONS

This study shows that Zn hyperaccumulation in *N. caerulescens* results in a myriad of changes in both elemental and metabolite profiles even though no change in growth rates is observed. The Zn hyperaccumulation resulted in changes to the galactolipids profile, producing lipids and signalling molecules that have only been seen in plants which have undergone mechanical wounding. This shows that Zn hyperaccumulation is not just a constitutive trait and that these lipid mediators are part of the signalling network in *N. caerulescens* which dynamically changes with Zn concentrations. Of the more than 2,000 metabolites analysed no single molecule stood out as the key Zn-binding compound which could account for the 2% Zn present in the leaf tissue showing that it is unlikely that nicotianamine or other small molecules are involved in storage of Zn and that they are more likely involved in the transport and re-distribution of micro-nutrients. There is still a need for improved analytical techniques which can accurately define the co-ordination chemistry *in vivo*. The lack of a clear highly selective metal-binding small molecule provides more weight to the hypothesis that an alternative mechanism of chelation and storage is occurring for example the co-ordination of Zn to the cell wall.

ACKNOWLEDGEMENTS

This research was funded by an early career researcher grant provided to Dr Callahan by The University of Melbourne. The authors are grateful for support from the Victorian Node of Metabolomics Australia which is funded through Bioplatforms Australia Pty Ltd from Federal Government grants to the NCRIS/CRIS/EIF programs, the Victorian State Government and the University of Melbourne. The authors declare no conflict of interest in this work.

REFERENCES

1. C. Anderson, A. Deram, D. Petit, R. Brooks, R. Stewart and R. Simcock, in *Trace Elements in Soil: Bioavailability, Flux, and Transfer*, eds. I. K. Iskandar and M. B. Kirkham, CRC Press, Boca Raton, 2001, ch. 4, pp. 63-76.
2. C. Chen, D. Huang and J. Liu, Functions and Toxicity of Nickel in Plants: Recent Advances and Future Prospects, *CLEAN – Soil, Air, Water*, 2009, 37, 304-313.
3. E. Gajewska, M. Wielanek, K. Bergier and M. Skłodowska, Nickel-induced depression of nitrogen assimilation in wheat roots, *Acta Physiologiae Plantarum*, 2009, 31, 1291-1300.
4. K. V. Madhava Rao and T. V. S. Sresty, Antioxidative parameters in the seedlings of pigeonpea (Cajanus cajan (L.) Millspaugh) in response to Zn and Ni stresses, *Plant Sci.*, 2000, 157, 113-128.
5. J. Molas, Changes of chloroplast ultrastructure and total chlorophyll concentration in cabbage leaves caused by excess of organic Ni(II) complexes, *Environ. Exp. Bot.*, 2002, 47, 115-126.
6. A. J. M. Baker, S. P. McGrath, R. D. Reeves and J. A. C. Smith, in *Phytoremediation of Contaminated Soil and Water*, eds. G. S. Bañuelos and N. Terry, Lewis Publishers, Boca Raton, 2000, pp. 85-107.
7. U. Krämer, Metal hyperaccumulation in Plants, *Annu. Rev. Plant Biol.*, 2010, 61, 517-534.
8. M. J. Milner and L. V. Kochian, Investigating heavy-metal hyperaccumulation using *Thlaspi caerulescens* as a model system, *Ann. Bot.*, 2008, 102, 3-13.
9. R. D. Reeves and A. J. M. Baker, in *Phytoremediation of Toxic Metals*, eds. I. Raskin and B. D. Ensley, J. Wiley, New York, 2000, pp. 193-229.
10. R. S. Boyd, in *Plants that Hyperaccumulate Heavy Metals*, ed. R. R. Brooks, CAB International, Oxford; New York, 1998, pp. 181-201.
11. M. Hanikenne and C. Nouet, Metal hyperaccumulation and hypertolerance: a model for plant evolutionary genomics, *Curr. Opin. Plant Biol.*, 2011, 14, 252-259.
12. N. S. Pence, P. B. Larsen, S. D. Ebbs, D. L. Letham, M. M. Lasat, D. F. Garvin, D. Eide and L. V. Kochian, The molecular physiology of heavy metal transport in the Zn/Cd hyperaccumulator *Thlaspi caerulescens*, *P.N.A.S.*, 2000, 97, 4956-4960.
13. A. G. L. Assunção, P. D. C. Martins, S. De Folter, R. Vooijs, H. Schat and M. G. M. Aarts, Elevated expression of metal transporter genes in three accessions of the metal hyperaccumulator *Thlaspi caerulescens*, *Plant, Cell Envir.*, 2001, 24, 217-226.
14. J.-E. Sarry, L. Kuhn, C. Ducruix, A. Lafaye, C. Junot, V. Hugouvieux, A. Jourdain, O. Bastien, J. B. Fievet, D. Vailhen, B. Amekraz, C. Moulin, E. Ezan, J. Garin and J. Bourguignon, The early responses of *Arabidopsis thaliana* cells to cadmium exposure explored by protein and metabolite profiling analyses, *Proteomics*, 2006, 6, 2180-2198.
15. J. Lee, R. D. Reeves, R. R. Brooks and T. Jaffré, The relation between nickel and citric acid in some nickel-accumulating plants, *Phytochemistry*, 1978, 17, 1033-1035.
16. D. E. Salt, R. C. Prince, A. J. M. Baker, I. Raskin and I. J. Pickering, Zinc ligands in the metal hyperaccumulator *Thlaspi caerulescens* as determined using x-ray absorption spectroscopy, *Environ. Sci. Technol.*, 1999, 33, 713-717.
17. U. Krämer, I. J. Pickering, R. C. Prince, I. Raskin and D. E. Salt, Subcellular localization and speciation of nickel in hyperaccumulator and non-accumulator *Thlaspi* species, *Plant Physiol.*, 2000, 122, 1343-1353.
18. H. Küpper, A. Mijovilovich, W. Meyer-Klaucke and P. M. H. Kroneck, Tissue- and age-dependent differences in the complexation of cadmium and zinc in the cadmium/zinc hyperaccumulator *Thlaspi caerulescens* (Ganges ecotype) revealed by X-ray absorption spectroscopy, *Plant Physiol.*, 2004, 134, 748-757.
19. D. L. Callahan, A. J. Baker, S. D. Kolev and A. G. Wedd, Metal ion ligands in hyperaccumulating plants, *J. Biol. Inorg. Chem.*, 2006, 11, 2-12.
20. G. Anderegg and H. Ripperger, Correlation between metal complex formation and biological activity of nicotianamine analogues, *J. Chem. Soc., Chem. Commun.*, 1989, 647-650.

21. A. E. Martell and R. D. Hancock, *Metal complexes in aqueous solutions*, Plenum Press, New York, 1996.
22. I. Beneš, K. Schreiber, H. Ripperger and A. Kircheiss, Metal complex formation by nicotianamine, a possible phytosiderophore, *Experientia*, 1983, 39, 261-262.
23. W. A. Peer, M. Mamoudian, B. Lahner, R. D. Reeves, A. S. Murphy and D. E. Salt, Identifying model metal hyperaccumulating plants: germplasm analysis of 20 Brassicaceae accessions from a wide geographical area, *New Phytol.*, 2003, 159, 421-430.
24. A. G. L. Assunção, H. Schat and M. G. M. Aarts, *Thlaspi caerulescens*, an attractive model species to study heavy metal hyperaccumulation in plants, *New Phytol.*, 2003, 159, 351-360.
25. J. E. Van De Mortel and M. G. M. Aarts, Comparative transcriptomics – model species lead the way, *New Phytol.*, 2006, 170, 199-201.
26. T. Schneider, D. P. Persson, S. Husted, M. Schellenberg, P. Gehrig, Y. Lee, E. Martinoia, J. K. Schjoerring and S. Meyer, A proteomics approach to investigate the process of Zn hyperaccumulation in *Noccaea caerulescens* (J & C. Presl) F.K. Meyer, *Plant J.*, 2013, 73, 131-142.
27. A. J. M. Baker, R. D. Reeves and A. S. M. Hajar, Heavy Metal accumulation and tolerance in British populations of the metallophyte *Thlaspi Caerulescens* J-and-C Presl (Brassicaceae), *New Phytol.*, 1994, 127, 61-68.
28. Z. G. Shen, F. J. Zhao and S. P. McGrath, Uptake and transport of zinc in the hyperaccumulator *Thlaspi caerulescens* and the non-hyperaccumulator *Thlaspi ochroleucum*, *Plant, Cell Environ.*, 1997, 20, 898-906.
29. S. O'Callaghan, D. De Souza, A. Isaac, Q. Wang, L. Hodkinson, M. Olshansky, T. Erwin, B. Appelbe, D. Tull, U. Roessner, A. Bacic, M. McConville and V. Likic, PyMS: a Python toolkit for processing of gas chromatography-mass spectrometry (GC-MS) data. Application and comparative study of selected tools, *BMC Bioinformatics*, 2012, 13, 115.
30. U. Roessner, A. Luedemann, D. Brust, O. Fiehn, T. Linke, L. Willmitzer and A. R. Fernie, Metabolic profiling allows comprehensive phenotyping of genetically or environmentally modified plant systems, *Plant Cell*, 2001, 13, 11-29.
31. C. Cosio, E. Martinoia and C. Keller, Hyperaccumulation of cadmium and zinc in *Thlaspi caerulescens* and *Arabidopsis halleri* at the leaf cellular level, *Plant Physiol.*, 2004, 134, 716-725.
32. S. N. Whiting, J. R. Leake, S. P. McGrath and A. J. M. Baker, Positive responses to Zn and Cd by roots of the Zn and Cd hyperaccumulator *Thlaspi caerulescens*, *New Phytol.*, 2000, 145, 199-210.
33. A. v. d. Ent, A. J. M. Baker, R. D. Reeves, A. J. Pollard and H. Schat, Hyperaccumulators of metal and metalloid trace elements: Facts and fiction, *Plant Soil*, 2013, 362, 319-334.
34. A. Ibrahim, A.-L. Schütz, J.-M. Galano, C. Herrfurth, K. Feussner, T. Durand, F. Brodhun and I. Feussner, The alphabet of galactolipids in *Arabidopsis thaliana*, *Front. plant sci.,* 2011, 2.
35. P. Dörmann and C. Benning, Galactolipids rule in seed plants, *Trends Plant Sci.*, 2002, 7, 112-118.
36. J. W. Fahey, A. T. Zalcmann and P. Talalay, The chemical diversity and distribution of glucosinolates and isothiocyanates among plants, *Phytochem.*, 2001, 56, 5-51.
37. S. Textor and J. Gershenzon, Herbivore induction of the glucosinolate–myrosinase defense system: major trends, biochemical bases and ecological significance, *Phytochem. Rev.*, 2009, 8, 149-170.
38. K. J. O'Callaghan, P. J. Stone, X. Hu, D. W. Griffiths, M. R. Davey and E. C. Cocking, Effects of glucosinolates and flavonoids on colonization of the roots of *Brassica napus* by *Azorhizobium caulinodans* ORS571, *App. Envir. Microbiol.*, 2000, 66, 2185-2191.
39. V. Neveu, J. Perez-Jiménez, F. Vos, V. Crespy, L. du Chaffaut, L. Mennen, C. Knox, R. Eisner, J. Cruz, D. Wishart and A. Scalbert, Phenol-Explorer: an online comprehensive database on polyphenol contents in foods, *Database*, 2010, 2010.
40. H. Irving and R. J. P. Williams, 637. The stability of transition-metal complexes, *J. Chem. Soc.*, 1953, 0, 3192-3210.
41. P. C. DeKock, Heavy-metal toxicity and iron chlorosis, *Ann. Bot.*, 1956, 20, 133-141.

42. U. Deinlein, M. Weber, H. Schmidt, S. Rensch, A. Trampczynska, T. H. Hansen, S. Husted, J. K. Schjoerring, I. N. Talke, U. Krämer and S. Clemens, Elevated nicotianamine levels in *Arabidopsis halleri* roots play a key role in zinc hyperaccumulation, *Plant Cell*, 2012, 24, 708-723.
43. M. J. Haydon, M. Kawachi, M. Wirtz, S. Hillmer, R. Hell and U. Krämer, Vacuolar nicotianamine has critical and distinct roles under iron deficiency and for zinc sequestration in *Arabidopsis*, *Plant Cell*, 2012, 24, 724-737.
44. B. A. Stelmach, A. Muller, P. Hennig, S. Gebhardt, M. Schubert-Zsilavecz and E. W. Weiler, A novel class of oxylipins, sn1-O-(12-oxophytodienoyl)-sn2-O-(hexadecatrienoyl)-monogalactosyl Diglyceride, from *Arabidopsis thaliana*, *J. Biol. Chem.*, 2001, 276, 12832-12838.
45. M. X. Andersson, M. Hamberg, O. Kourtchenko, A. Brunnstrom, K. L. McPhail, W. H. Gerwick, C. Gobel, I. Feussner and M. Ellerstrom, Oxylipin profiling of the hypersensitive response in *Arabidopsis thaliana*. Formation of a novel oxo-phytodienoic acid-containing galactolipid, arabidopside E, *J. Biol. Chem.*, 2006, 281, 31528-31537.
46. C. Bottcher and E. W. Weiler, cyclo-Oxylipin-galactolipids in plants: occurrence and dynamics, *Planta*, 2007, 226, 629-637.
47. C. M. Buseman, P. Tamura, A. A. Sparks, E. J. Baughman, S. Maatta, J. Zhao, M. R. Roth, S. W. Esch, J. Shah, T. D. Williams and R. Welti, Wounding stimulates the accumulation of glycerolipids containing oxophytodienoic acid and dinor-oxophytodienoic acid in *Arabidopsis* leaves, *Plant Physiol.*, 2006, 142, 28-39.
48. Y. Hisamatsu, N. Goto, K. Hasegawa and H. Shigemori, Arabidopsides A and B, two new oxylipins from *Arabidopsis thaliana*, *Tetrahedron Lett.*, 2003, 44, 5553-5556.
49. Y. Hisamatsu, N. Goto, K. Hasegawa and H. Shigemori, Senescence-promoting effect of arabidopside A, *Z Naturforsch C*, 2006, 61, 363-366.
50. O. Kourtchenko, M. X. Andersson, M. Hamberg, A. Brunnstrom, C. Gobel, K. L. McPhail, W. H. Gerwick, I. Feussner and M. Ellerstrom, Oxo-phytodienoic acid-containing galactolipids in *Arabidopsis*: jasmonate signaling dependence, *Plant Physiol.*, 2007, 145, 1658-1669.
51. C. Wasternack and B. Hause, Jasmonates: biosynthesis, perception, signal transduction and action in plant stress response, growth and development. An update to the 2007 review in Annals of Botany, *Ann. Bot.*, 2013, 111, 1021-1058.
52. H. N. Fones, C. J. Eyles, M. H. Bennett, J. A. C. Smith and G. M. Preston, Uncoupling of reactive oxygen species accumulation and defence signalling in the metal hyperaccumulator plant *Noccaea caerulescens*, *New Phytol.*, 2013, 199, 916-924.
53. M. Llugany, S. R. Martin, J. Barcelo and C. Poschenrieder, Endogenous jasmonic and salicylic acids levels in the Cd-hyperaccumulator *Noccaea* (*Thlaspi*) *praecox* exposed to fungal infection and/or mechanical stress, *Plant Cell Rep.*, 2013, 32, 1243-1249.
54. R. P. Tolrà, C. Poschenrieder and J. Barceló, Zinc hyperaccumulation in *Thlaspi caerulescens*. II. Influence on organic acids, *J. Plant Nutr.*, 1996, 19, 1541-1550.
55. M. Wójcik, E. Skórzyńska-Polit and A. Tukiendorf, Organic acids accumultion and antioxidant enzyme activities in *Thlaspi caerulescens* under Zn and Cd stress, *Plant growth and regulation*, 2006, 48, 145.
56. T. Taji, C. Ohsumi, S. Iuchi, M. Seki, M. Kasuga, M. Kobayashi, K. Yamaguchi-Shinozaki and K. Shinozaki, Important roles of drought- and cold-inducible genes for galactinol synthase in stress tolerance in *Arabidopsis thaliana*, *Plant J.*, 2002, 29, 417-426.
57. B. J. Shelp, A. W. Bown and M. D. McLean, Metabolism and functions of gammaaminobutyric acid, *Trends Plant Sci.*, 1999, 4, 446-452.
58. C. Masclaux-Daubresse, M. H. Valadier, E. Carrayol, M. Reisdorf-Cren and B. Hirel, Diurnal changes in the expression of glutamate dehydrogenase and nitrate reductase are involved in the C/N balance of tobacco source leaves, *Plant, Cell Environ.*, 2002, 25, 1451-1462.
59. H. Renault, V. Roussel, A. El Amrani, M. Arzel, D. Renault, A. Bouchereau and C. Deleu, The *Arabidopsis* pop2-1 mutant reveals the involvement of GABA transaminase in salt stress tolerance, *BMC Plant Biol.*, 2010, 10, 1-16.

60. D. L. Callahan, S. D. Kolev, R. A. J. O'Hair, D. E. Salt and A. J. M. Baker, Relationships of nicotianamine and other amino acids with nickel, zinc and iron in *Thlaspi hyperaccumulators*, *New Phytol.*, 2007, 176, 836-848.
61. S. Shojima, N. Nishizawa, S. Fushiya, S. Nozoe, T. Kumashiro, T. Nagata, T. Ohata and S. Mori, Biosynthesis of nicotianamine in the suspension-cultured cells of tobacco (Nicotiana megalosiphon), *Biology of Metals*, 1989, 2, 142-145.
62. H. Küpper, F. Jie Zhao and S. P. McGrath, Cellular compartmentation of zinc in leaves of the hyperaccumulator *Thlaspi caerulescens*, *Plant Physiol.*, 1999, 119, 305-312.
63. R. Rellán-Álvarez, J. Abadía and A. Álvarez-Fernández, Formation of metal-nicotianamine complexes as affected by pH, ligand exchange with citrate and metal exchange. A study by electrospray ionization time-of-flight mass spectrometry, *Rapid Commun. Mass Spectrom.*, 2008, 22, 1553-1562.
64. M. J. Haydon and C. S. Cobbett, Transporters of ligands for essential metal ions in plants, *New Phytol.*, 2007, 174, 499-506.
65. Z. Xiao, J. Brose, S. Schimo, S. M. Ackland, S. La Fontaine and A. G. Wedd, Unification of the Copper(I) binding affinities of the metallo-chaperones Atx1, Atox1, and related proteins: detection probes and affinity standards, *J. Biol. Chem.*, 2011, 286, 11047-11055.

SUPPORTING INFORMATION ABBREVIATED LEGENDS

Figure S1: Positive ion internal standard area by injection order

Figure S2: Leaf fresh mass of sixteen week old *N. caerulescens* plants

Figure S3: Principal components analysis of the negative ion dataset

Figure S4: Principal components analyses of the GC-MS data

Table S1: Concentrations of hydroponic nutrients.

Table S2: The full LC-MS and GC-MS data datasets.

Table S3: Metabolites from GC-MS data set which had significantly different changes between treatment groups and control.

Figure 1: *N. caerulescens* plants after 8 weeks of Zn treatment; front left control (5 µM Zn); back left 50 µM Zn; front right 250 µM Zn; back right 500 µM Zn.

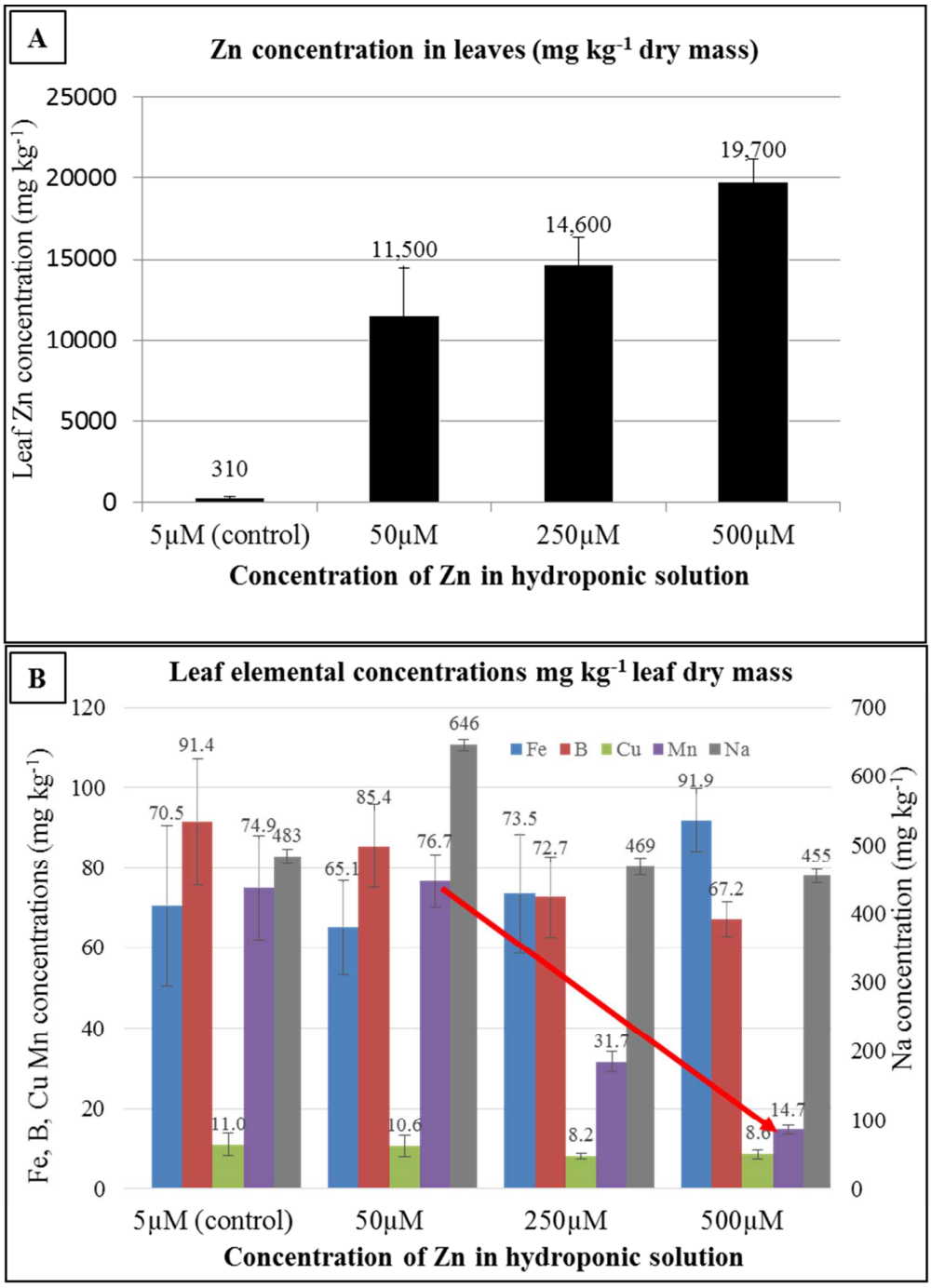

Figure 2: The elemental concentrations measured by ICP-OES in dried leaf tissues of *N. caerulescens* plants grown in hydroponic solutions with four different Zn concentrations 5, 50, 250 and 500 µM. (A) The mean Zn concentrations (mg/kg dry mass; n=10 plants per treatment), note the error bars represent standard deviation; (B) mean Fe, B, Cu, Mn and Na concentrations (mg/kg dry mass; n=10) in the same leaf tissue. The diagonal red arrow highlights the large decrease in Mn concentration. Please note that Na is plotted on a different scale.

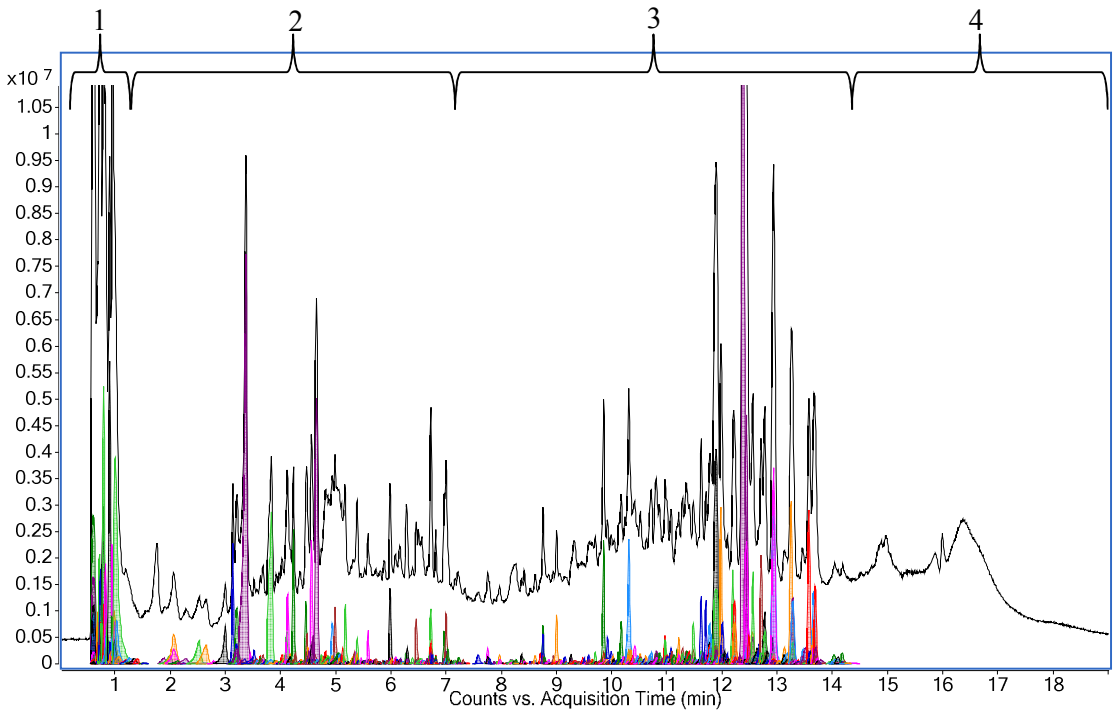

Figure 3: A positive ion total ion chromatogram (TIC) of a reversed phase C-18 HPLC profile from *N. caerulescens* leaf extracts. The blank trace is the TIC with the molecular features shown in colour. In this trace 1,791 features were found. The regions of typical eluting compounds are also shown, region 1: polar fraction including organic acids, polar amino acids, sugars, Zn-complexes, 2: non-polar amino acids di-peptides, secondary metabolites such as glucosinolates, polyphenols, 3: lipids such as galactolipids (high abundant peaks) free fatty acids, polar phospholipids, 4 column wash and re-equilibration.

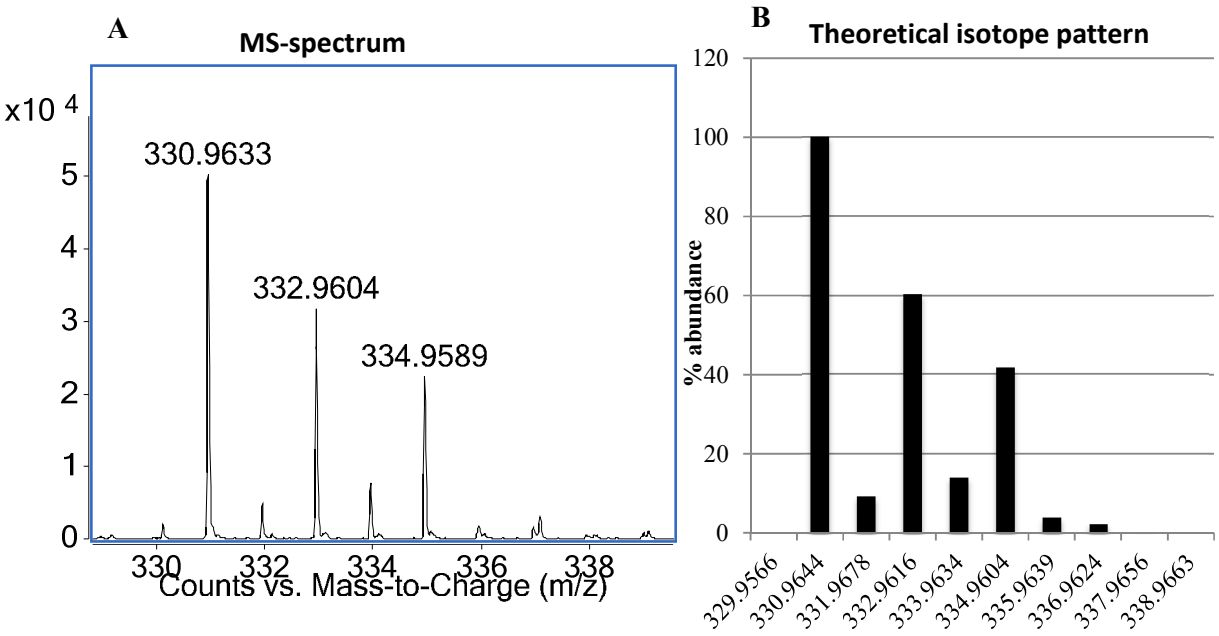

Figure 4: (A) Zn-malonate complex $[Zn^{2+}(Mal\text{-}H^{+})^{-}(Mal)]^{+}$ detected by LC-MS in the leaf extract of a 500 µM Zn treated plant; (B) theoretical isotope pattern for $[Zn(C_8H_{11}O_{10})]^{+}$. Note, detection in the MS does not necessarily represent an *in-vivo* complex as these complexes can form in the ionization source.

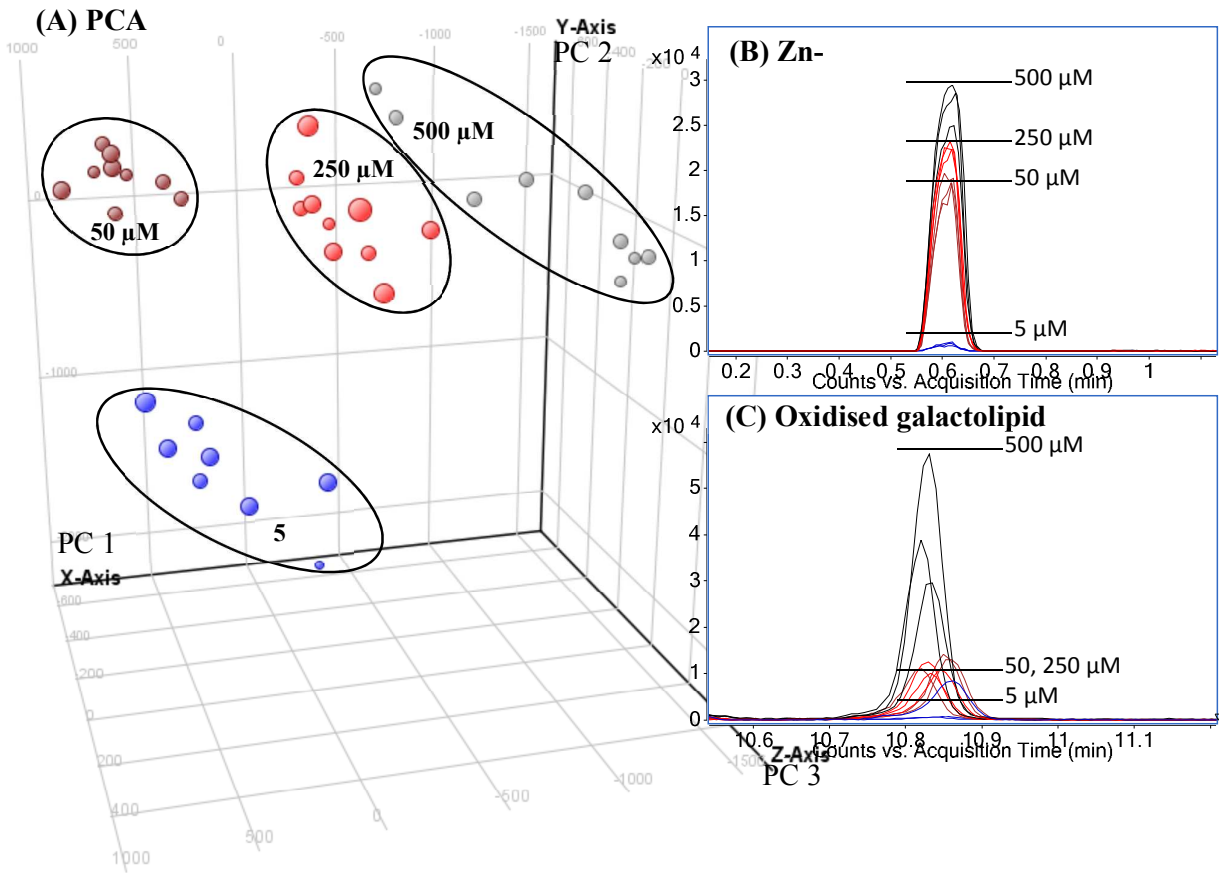

Figure 5: (A) A principal components analysis (PCA) of the positive ion dataset showing distinct clusters for the different treatment groups (PC - principal component number); (B) overlaid extracted ion chromatogram of the an unidentified Zn-complex; (C) overlaid extracted ion chromatogram of oxidised galactolipids putatively identified as (HPOT/ketol-18:2)/16:3-MGDG (Ibrahim et al. 2011).

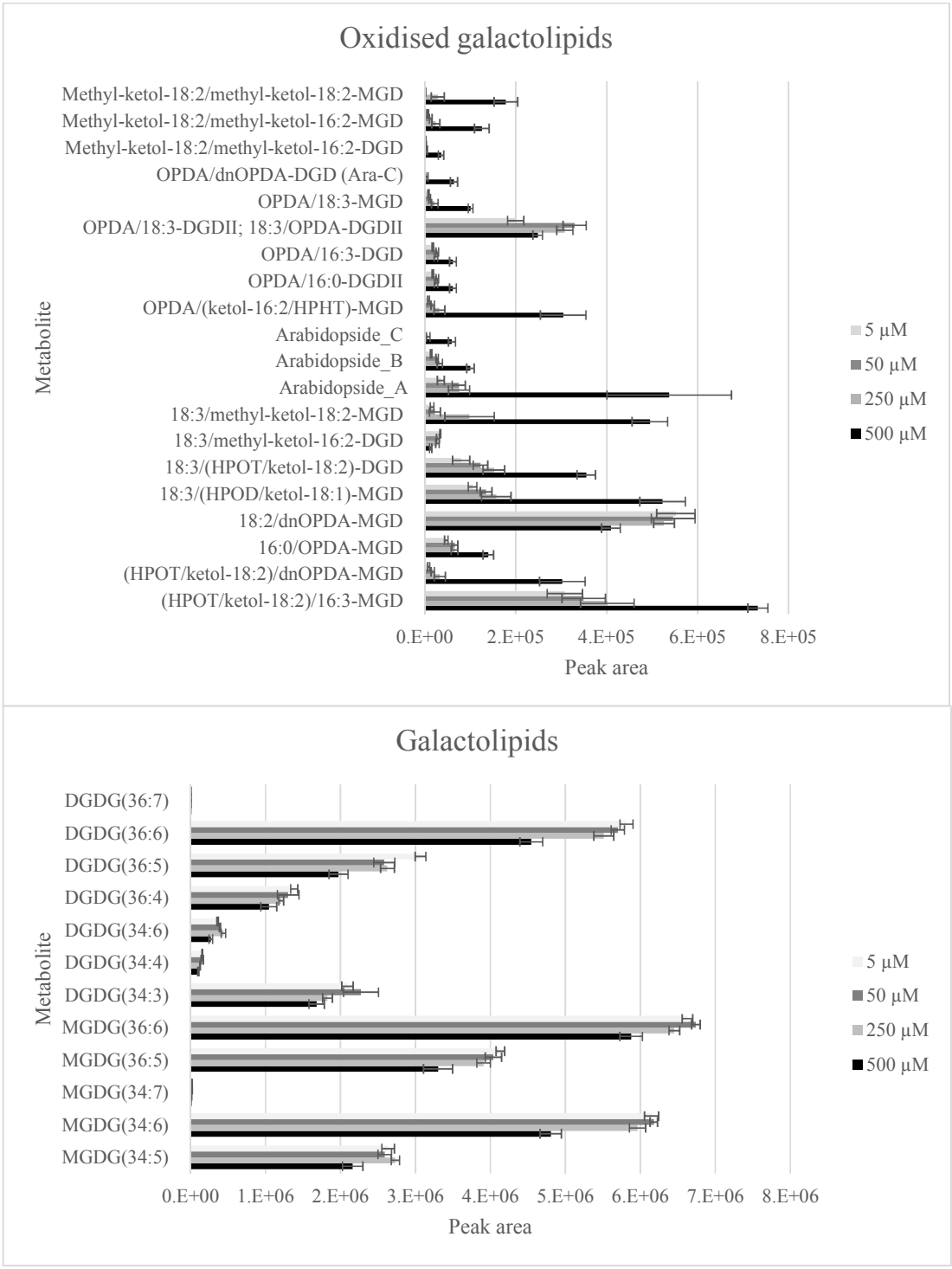

Figure 6: Statistically significant changes ($p<0.05$) in the galactolipid levels detected in the positive ion LC-MS dataset which have shown a change with treatment of Zn, error bars represent standard deviation (n=8-10). An obvious decrease in galactolipids (bottom) and an increase the oxidised galactolipids (top) can be observed in the different treatment groups.

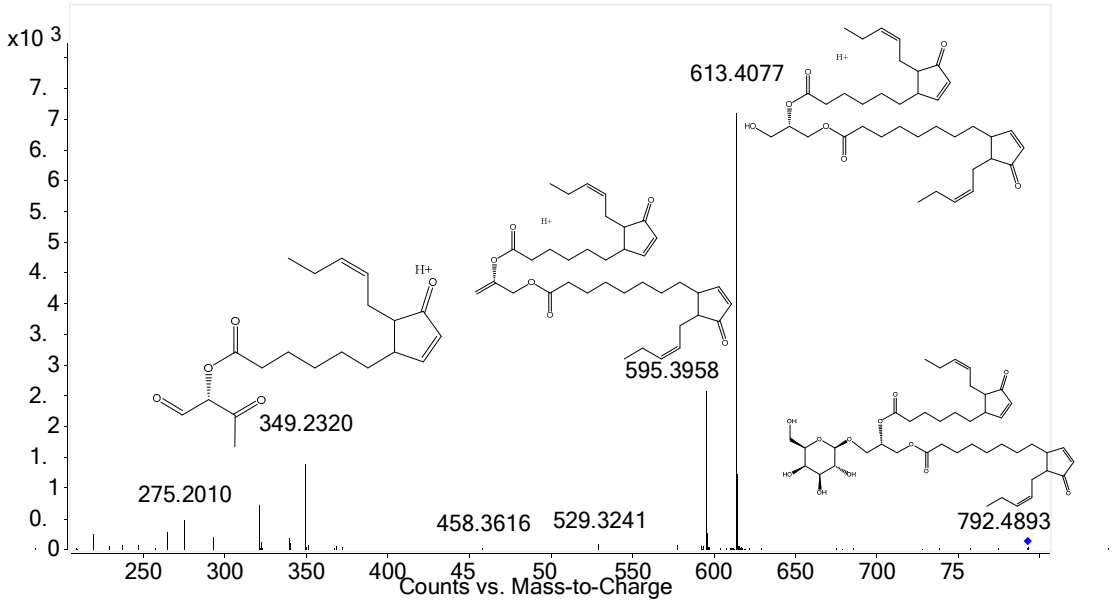

Figure 7: An MS/MS spectrum of arabidopside A with an *m/z* 792.4893, $[C_{43}H_{66}O_{12}+NH_4^+]^+$. Structures of key product ions at *m/z* 613, 595, 349 are shown. These corresponds to $[M+H^+]^+$ ions containing 12-oxo-10,15-phytodienoic acid, an oxidised fatty acid and thus confirms the structure as Arabisopside A. These fragment ions agree with other published MS/MS data (Ibrahim et al 2011).

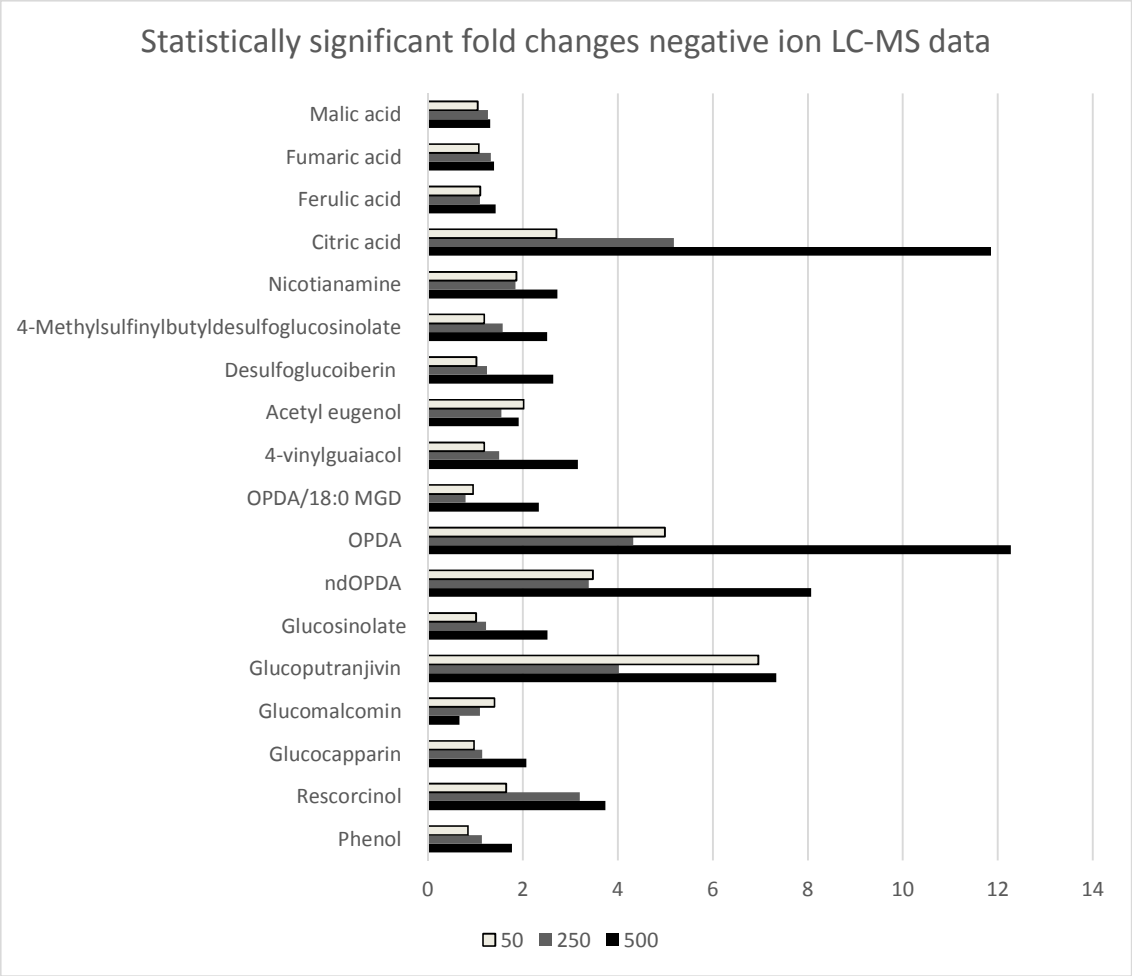

Figure 8: Metabolites with statistically significant fold changes in relation to the control plants ($p<0.05$) of identified glucosinolates and organic acids in the negative ion LC-MS data. Data represented as fold changes as opposed to peak area values due to the very different concentrations of the metabolites graphed.